ChemComm

COMMUNICATION

View Article Online
View Journal | View Issue

Cite this: *Chem. Commun.*, 2025, **61**, 17609

Received 31st July 2025,
Accepted 9th October 2025

DOI: 10.1039/d5cc04393j

rsc.li/chemcomm

Konjac glucomannan derived biodegradable superionic solid-state electrolyte films for devising economically viable supercapacitor

Sushant Wakekar, [a] Laxmi Pasupuleti, [a] Bapan Jana, [b] Saisrinu Yarramsetti, [a] Pardha Saradhi Maram, [a] Maheswaran Shanmugam, [b] Laxmi Narayana Patro [c] and Chinmoy Das *[a]

We synthesized biodegradable and economically viable solid-state electrolyte films based on konjac glucomannan (KG) and sodium iodide (NaI). Among the KG_{NaI-x} (x = 31–69 wt%) films, KG_{NaI-69} exhibits superior flexibility, biodegradability, and sodium superionic conductivity of 77.9 mS cm^{-1}. The KG_{NaI-69}-based supercapacitor delivers outstanding electrochemical efficiency and cycling stability, retaining 84.4% capacitance after 5000 cycles establishing its potentiality toward flexible energy storage devices.

In recent years, supercapacitors have attracted widespread interest as next-generation energy storage devices owing to their superior power density, rapid charge–discharge rates, and remarkable life cycle compared to conventional batteries.[1] To complement these advantages, the development of environmentally friendly and efficient electrolytes is crucial. In this regard, solid biopolymer electrolytes have emerged as a promising class of materials, offering a viable alternative to traditional liquid electrolytes and synthetic solid polymer electrolytes.[2] These natural polymer-based systems not only overcome the leakage and volatility issues associated with liquid electrolytes but also provide mechanical flexibility, thermal stability, and environmental safety.[3] Unlike synthetic polymers such as polyethylene oxide (PEO),[4] polyvinylidene fluoride (PVDF),[5] and others, which are derived from petrochemical sources, biopolymer electrolytes[6–8] sourced from natural materials offer several intrinsic advantages. These include smooth handling, ease of film casting, non-toxicity, and inherent biodegradability, making them highly suitable for disposable electronics.[9] Over the last decade, increasing attention has been directed towards exploring the potential of natural polymers owing to their sustainable origins, low environmental footprint, biocompatibility, and renewability. Among various biopolymers, konjac glucomannan (KG) has emerged as a particularly attractive candidate as it is a naturally occurring, water-soluble polysaccharide extracted from the tuber of the konjac plant, consisting of β-1,4-linked D-mannose and D-glucose units with acetyl side chains.[10] The high-water absorption capacity, film-forming ability, and non-toxic nature of KG make it suitable as a matrix for ion transport.[11] In recent developments, KG has been successfully employed as a host matrix in the fabrication of solid-state electrolytes toward the fabrication of batteries[12] and supercapacitors.[13] These findings indicate that KG hold a considerable potential for the next-generation sustainable, and high-performance electrochemical energy storage devices, however the key challenge remains in elevating ionic conductivity above 10 mS cm^{-1} at room temperature.

Herein, we aim to synthesize a series of Na^+-ion based novel solid-state electrolyte films (KG_{NaI-x}; x = 31, 48, 58, 65, and 69 wt%) for economically viable and sustainable supercapacitors. Among various compositions, KG_{NaI-69} film was tested for environmental compatibility through the rapid, enzyme-free degradation in aqueous medium across a range of pH conditions (acidic, neutral, and basic) for biodegradable and ecofriendly material. The KG_{NaI-69} film exhibited sodium superionic conductivity of 77.9 mS cm^{-1} for developing sustainable supercapacitor device. KG_{NaI-x} (x = 31, 48, 58, 65, and 69 wt%) solid-state electrolyte films were synthesized *via in situ* gelation of konjac glucomannan and sodium iodide in distilled water with varying weight ratios of NaI (Fig. 1a, Fig. S1 and Table S1). We characterized the transparent films through powder X-ray diffraction (PXRD) analysis to identify the structure of the composite films (Fig. 1b and Fig. S2). The PXRD pattern of pristine NaI showed strong and sharp diffraction peaks, indicative of its highly crystalline nature (Fig. S3). In contrast, KG exhibits a broad and diffusedly scattered diffraction pattern typical of an amorphous structure.[14] Interestingly, all the synthesized KG_{NaI} films showed broad and diffusedly scattered patterns at ambient conditions (Fig. S2a). The absence of crystalline patterns in different regions of the KG_{NaI-69} film indicates the formation of a homogeneous phase (Fig. S2b).

[a] *Department of Chemistry, SRM University – AP, Amaravati, Andhra Pradesh – 522240, India. E-mail: chinmoy.d@srmap.edu.in*
[b] *Department of Chemistry, Indian Institute of Technology Bombay, Powai, Mumbai, Maharashtra – 400076, India*
[c] *Department of Physics, SRM University – AP, Amaravati, Andhra Pradesh – 522240, India*

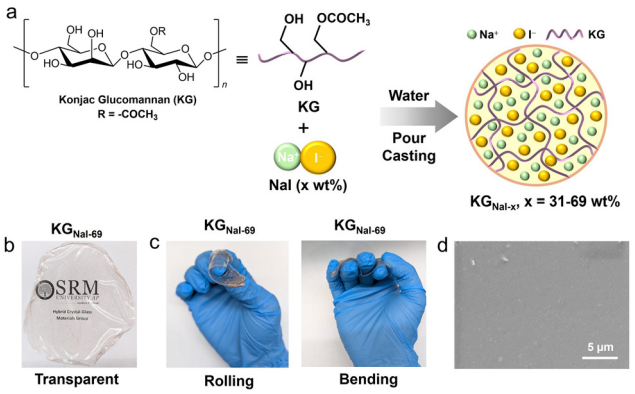

Fig. 1 (a) Synthetic scheme for the preparation of solid-state electrolyte films (KG_{NaI-x}; x = 31–69 wt%). (b) An image of a representative transparent film of KG_{NaI-69}. (c) Photographs of two different modes of flexibility of a representative KG_{NaI-69} film. (d) Scanning electron microscope image of KG_{NaI-69} film. Scale bar: 5 µm.

Further, the structural characteristics of KG_{NaI-x} (x = 31–69 wt%) were analysed using Fourier transform infrared (FT-IR) spectroscopy (Fig. S4). Broad absorption bands were observed around 3295 cm^{-1} and 2883 cm^{-1}, corresponding to the stretching vibrations of hydroxyl (–OH) and C–H bonds of methyl groups, respectively. Additionally, characteristic bands attributed to the β-1,4 glycosidic linkage in mannose units were identified at around 870 cm^{-1} and 798 cm^{-1}.[14] A prominent peak at 1600 cm^{-1} was assigned to the H–O–H bending vibration. Upon incorporation of NaI into the KG matrix, a notable increase in the intensity of the band near 1600 cm^{-1} was observed. This enhancement indicates possible interactions between Na^+ ions and the −OH or C–O functional groups of the polysaccharide chains, suggesting the formation of bonds between them.[8] The interactions likely contribute to the structural stability and uniformity of the resulting composite films. Moreover, CHN elemental analysis showed a gradual decrease in the percentages of carbon (% C) and hydrogen (% H) with increasing NaI content in the films, resembling the compositional shift in accordance with the synthesis approach (Table S2). SEM analysis of the KG_{NaI-x} (x = 31, 48, 58, 65, and 69 wt%) films exhibit smooth surfaces, indicating amorphous characteristics (Fig. 1d and Fig. S5). In addition, EDAX analysis confirms a progressive increase in Na^+ ion concentration with the increasing NaI content used during solid-state electrolyte films preparation (Fig. S6). The KG_{NaI-x} (x = 31–69 wt%) films show significant structural stability, primarily maintained by hydrogen bonding within the water-assisted network.[15]

KG_{NaI-x} (x = 31, 48, 58, 65, and 69 wt%) films were activated at 105 °C for 10 hours to investigate the thermal stability of the dehydrated films. Thermogravimetric analysis (TGA) of thermally activated films remained stable up to 208–237 °C based on the incorporation of various concentrations of NaI (Fig. S7). As the NaI content increased, a gradual reduction of thermal stability was observed, attributed to the decreasing polysaccharide content in the network. Beyond the thermally stable region, the films experienced weight loss due to the breakdown of glycosidic bonds in the polysaccharide backbone, generating monomeric units that promote further degradation. A complete decomposition of the films occurred above 500 °C, primarily through pyrolysis.[16] To understand the polymeric chain dynamics, we performed differential scanning calorimetry (DSC) on the dehydrated KG_{NaI-x} films (x = 31, 48, 58, and 65 wt%). The glass transition temperatures (T_g) were observed around 80–102 °C during first heating scans for the films with different NaI-content, corresponding to the relaxation of internal stresses as the polymer approaches thermodynamic equilibrium. Contrarily, KG_{NaI-69} showed two distinct glass transition temperatures (T_g) appeared at 114 °C and 124 °C while heating during first upscan, indicating microphase separation into NaI-rich and NaI-deficient domains with differing chain dynamics.[17,18] Additionally, KG_{NaI-69} film exhibited exothermic peaks between 150–200 °C, likely due to the crystallization of NaI-rich regions (Fig. S8), which is supported by PXRD analysis of thermally activated KG_{NaI-69} film (Fig. S3).

To evaluate biodegradability, KG_{NaI-69} film was immersed into aqueous solutions at pH 3, 7, and 12 under continuous stirring. The films gradually disintegrated into fibrils due to enhanced interaction with water, which facilitated hydrolysis of the solid-state electrolyte (Fig. 2 and Fig. S9). Complete disintegration of the film was observed within 2 hours in acidic and basic environments, while neutral pH conditions required *ca.* 5 hours. The accelerated breakdown under extreme pH conditions is attributed to the acid or base-catalysed cleavage of β-1,4-glycosidic bonds in the KG backbone. Acidic (pH 3) media promote protonation of glycosidic oxygen atoms, weakening the linkage, whereas basic (pH 12) conditions enhance nucleophilic attack *via* hydroxide ions.[19] Additionally, the amorphous nature of the composite film facilitates water uptake and chain mobility, further accelerating hydrolysis.[20] These results highlight the film's potential for rapid, enzyme-free biodegradation under environmentally relevant conditions, supporting its suitability for sustainable materials. The mechanical properties of solid-state electrolytes are critical indicators of their structural integrity. The mechanical properties of KG_{NaI-31} and KG_{NaI-69} films vary significantly with NaI content. KG_{NaI-31} exhibits a rigid and brittle features, marked by a high tensile strength and a Young's modulus of *ca.* 167 MPa (Fig. 1c, 3a, b and Fig. S10). In contrast, KG_{NaI-69} shows remarkable flexibility, with a lower tensile strength and a Young's modulus of *ca.* 0.02 MPa, with an impressive elongation at break of 310% contrast to 14% for KG_{NaI-31},

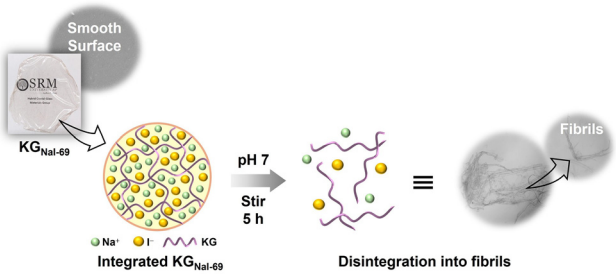

Fig. 2 Schematic representation for the biodegradability test of KG_{NaI-69}. Optical microscope image of KG_{NaI-69} film (10× magnification) after immersing into aqueous medium (pH 7, stir at 200 rpm, 5 h).

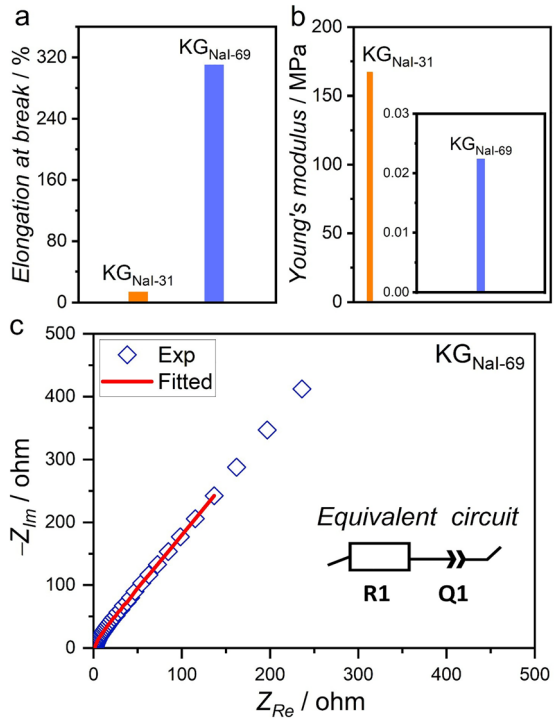

Fig. 3 (a) Comparison plot of elongation at break (%) for KG_{NaI-31} and KG_{NaI-69} films. (b) Comparison of Young's modulus (MPa) of KG_{NaI-31} and KG_{NaI-69} (inset) films. (c) The Nyquist plot of KG_{NaI-69}. Z_{Re} and Z_{Im} are the real and imaginary components, respectively. Inset: The red line indicates the fitting of electrochemical impedance data by using the specified equivalent circuit.

indicating high ductility (Fig. 3a, b and Fig. S10). The reduction of mechanical strength with increasing NaI content is likely due to the disruption of the KG chain orientation and decreased polymer mobility caused by Na^+ ions and polysaccharide interactions. Nevertheless, the tensile stress and strain values remain comparable to those reported for a flexible supercapacitor.[21]

To assess the ionic conductivity of KG_{NaI-x} (x = 31, 48, 58, 65, and 69 wt%) films, electrochemical impedance spectroscopy (EIS) was carried out across samples with varying Na^+ concentrations. The analysis indicated a gradual increase in ionic conductivity with increasing wt% of NaI, reaching 77.9 mS cm^{-1} at room temperature for the KG_{NaI-69} composition (Fig. 3c and Fig. S11), indicating sodium superionic conductivity (Table S3). This enhancement is largely driven by the water molecules within the polysaccharide network, which create hydrated channels.[22] These water channels facilitate Na^+ ion mobility *via* hydrogen-bond-mediated transport, contributing significantly to the overall conductivity of the films.[13,23] To understand the role of water molecules for the fast transport of Na^+-ion, we studied ionic conductivities in pre-activated sample (at 105 °C for 10 hours) of KG_{NaI-69} film (Fig. S12 and Table S4) and temperature dependent as-synthesized sample of KG_{NaI-69} film (Fig. S13 and Table S5). We found that the ionic conductivity of as-synthesized KG_{NaI-69} film exhibited 10^4–10^5 times higher than that of thermally pre-activated and gradually dehydrated KG_{NaI-69} film. Interestingly, KG_{NaI-69} exhibits the highest ionic conductivity, greatly surpassing konjac glucomannan–zinc acetate (0.6 mS cm^{-1})[12] and even the HPMC/KGM/NaI matrix (2.77 mS cm^{-1}),[13] underscoring its remarkable performance. The KG_{NaI-69} film exhibits an exceptionally high ionic transference number (t_{ion} ≈ 0.999), indicating that conduction is almost entirely ionic (Fig. S14). Furthermore, dielectric and conductivity analyses reveal suppressed interfacial polarization, enhanced ion mobility, and frequency-dependent transport (Fig. S15), suggesting the superior electrochemical performance of KG_{NaI-69}.[8] The electrochemical stability window (ESW) of the KG_{NaI-69} film was assessed through linear sweep voltammetry (LSV) using a SS|KG_{NaI-69}|SS cell configuration. The voltage was applied from 0 to 3 V at a scan rate of 0.1 V s^{-1}. A distinct increase in current was observed around 2.2 V in KG_{NaI-69} (Fig. S16), indicating the electrolyte degradation, suggesting possible ionic dissociation or interfacial instability beyond this voltage, marking the upper limit of its stable operating window.[6] Noticeably, NaI concentration also influences the ESW as the NaI content increases, a clear narrowing of the ESW is observed decreasing from 2.5 V (31 wt%) to 2.2 V (69 wt%). The decrease in ESW is likely due to the oxidation of iodide ions into molecular iodine (I_2) at relatively low potentials, leading to an earlier rise in faradaic current and diminishing oxidative stability.[15,24]

The electrochemical performance of KG_{NaI-69} as a solid-state electrolyte was evaluated using cyclic voltammetry (CV) and galvanostatic charge–discharge (GCD) with symmetric supercapacitor (Fig. 4a). The CV curves exhibited a typical leaf-like shape without redox peaks (Fig. S17), characteristic of electrochemical double-layer capacitance (EDLC). As the scan rate increased from 20 mV s^{-1} to 100 mV s^{-1}, a gradual rise in current was observed. The consistent shape of the curves at higher scan rates indicates low internal resistance, enabling efficient charge transfer and ion diffusion. Additionally, the minimal distortion in the curves suggests a stable electrode–electrolyte interface that facilitates rapid ion adsorption and desorption, reducing resistance and diffusion-related limitations.[25] GCD was performed at current densities of 1, 2, and 3 A g^{-1}, showing characteristic capacitive behaviour (Fig. 4a). The specific capacitance (C_{sp}) calculated to be 125, 52, and 12 F g^{-1} at the 1, 2, and 3 A g^{-1} current densities, respectively. A progressive increase in iR_{drop} with higher current densities indicates elevated ion transport resistance and interfacial losses, leading to diminished charge storage efficiency and reduced discharge times.[26] The corresponding energy densities were 17.3, 7.2, and 1.6 Wh kg^{-1}, while the associated power densities were 500, 997, and 1494 W kg^{-1} at

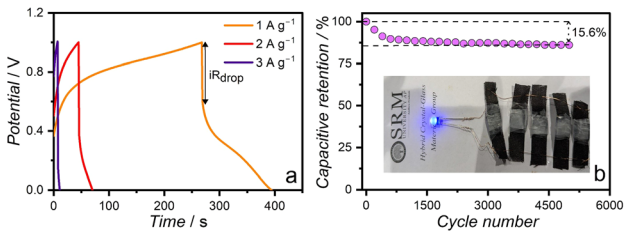

Fig. 4 (a) Galvanostatic charge–discharge measurement for KG_{NaI-69}. (b) Cyclic Stability at the current density of 5 A g^{-1}. Inset: digital image showing five parallelly connected supercapacitors powering a single blue LED.

1, 2, and 3 A g^{-1}, respectively. Examining the long-term stability of $KG_{NaI\text{-}69}$, charge–discharge cycling was performed up to 5000 cycles (Fig. 4b). The specific capacitance gradually decreased but retained 84.4% of its initial value, which demonstrates excellent durability and long cycle stability. The slight performance loss is likely due to electrolyte depletion and the formation of a charge depletion layer during early cycles, where some ions become trapped in the electrode's porous structure, reducing mobile charge carriers. This creates a depletion region at the electrode–electrolyte interface, lowering effective capacitance. Minor electrode degradation and slow interfacial structural changes may also contribute.[26] Despite these factors, the $KG_{NaI\text{-}69}$ solid electrolyte maintains high capacitance retention and feasible long-term reliability.

To conclude, we have developed a series of economically viable biopolymer-based KG_{NaI} films by incorporating sodium iodide into a konjac glucomannan polysaccharide host, representing a significant step forward in biodegradable solid-state electrolytes for sustainable energy storage applications (Table S6). Structural analyses confirm a uniform and homogeneous amorphous structure ensuring fast ion transport and mechanical integrity. Importantly, the film is inherently biodegradable, undergoing complete enzyme-free degradation within 2–5 hours across a broad pH range (3, 7, and 12). The optimized $KG_{NaI\text{-}69}$ composition exhibits excellent superionic conductivity of 77.9 mS cm^{-1} at room temperature, and a wide electrochemical stability window of 2.2 V, making it highly suitable for supercapacitor applications. A symmetric supercapacitor comprising of $KG_{NaI\text{-}69}$ film delivers an energy density of 17.36 Wh kg^{-1} and a power density of 500 W kg^{-1} at a current density of 1 A g^{-1} (Table S7). Galvanostatic charge–discharge tests demonstrate strong cycling durability, with 84.4% capacitance retention over 5000 cycles, highlighting its potential as a robust material for next-generation sustainable electronics. The rapid degradation of $KG_{NaI\text{-}69}$ film offers a distinct advantage for designing device for short-term operation and disposable energy devices, particularly it will provide the feasible remedy for reducing long-standing electronic waste disposal issues.

C. D. designed the project. S. W. carried out all the material synthesis and characterized the samples by PXRD, and FT-IR. B. J. and M. S. performed the TGA and DSC measurements, and C. D. and S. W. analysed the data. C. D., S. W., and L. P. analysed the mechanical properties, SEM and EDAX spectroscopic data. S. W., S. Y., L. N. P., and P. S. M. carried out all electrochemical characterization and analysed the data. C. D. and S. W. drafted the initial manuscript. All authors contributed to revising the manuscript. All authors have given approval to the final version of the manuscript.

This work was supported by the generous funding support from the SRM University-AP through the SEED grant (Sanction order no. SRMAP/URG/SEED/2023-24/019), and Anusandhan National Research Foundation (ANRF), Govt. of India sponsored PM-ECRG grant (Sanction order no. ANRF/ECRG/2024/001345/CS).

Conflicts of interest

There are no conflicts of interest to declare.

Data availability

The data supporting this article have been included as part of the supplementary information (SI). Supplementary information: PXRD, FT-IR, SEM/EDAX, TGA-DTA, DSC, EIS, and other electrochemical studies. See DOI: **https://doi.org/10.1039/d5cc04393j**.

Notes and references

1 G. P. Pandey, T. Liu, C. Hancock, Y. Li, X. S. Sun and J. Li, *J. Power Sources*, 2016, **328**, 510.
2 S. Majumdar, P. Sen and R. Ray, *J. Solid State Electrochem.*, 2022, 527–547.
3 H. Li, J. Yang, S. Chen, Z. Xu, J. Wang, Y. Nuli, Y. Guo and C. Liang, *Chem. Eng. J.*, 2021, **410**, 128415.
4 Y.-J. Li, C.-Y. Fan, J.-P. Zhang and X.-L. Wu, *Dalt. Trans.*, 2018, **47**, 14932–14937.
5 P. Li, Y. Huang, Y. Yu, X. Ma, Z. Wang and G. Shao, *J. Power Sources*, 2025, **628**, 235855.
6 R. T. Abdulwahid, S. B. Aziz and M. F. Z. Kadir, *Mater. Today Sustainable*, 2023, **23**, 100472.
7 C. D. D. Sundari, J. Karunawan, S. P. Santosa, I. M. Arcana and F. Iskandar, *ACS Appl. Polym. Mater.*, 2023, **5**, 6817–6827.
8 K. Jayalakshmi, S. Hegde and J. Monteiro, *J. Energy Storage*, 2024, **89**, 111575.
9 G. Gopinath, S. Ayyasamy, P. Shanmugaraj and R. Swaminathan, *J. Energy Storage*, 2023, **70**, 108065.
10 D. U. Kapoor, H. Sharma, R. Maheshwari, A. Pareek, M. Gaur, B. G. Prajapati, G. R. Castro, K. Thanawuth, S. Suttiruengwong and P. Sriamornsak, *Carbohydr. Polym.*, 2024, **339**, 122266.
11 C. Chandarana, S. Bonde, V. Vashi, M. S. Akhter and B. Prajapati, *J. Food Proc. Eng.*, 2024, **47**, e70009.
12 N. Chiaoprakobkij, M. Okhawilai, P. Kasemsiri and H. Uyama, *Int. J. Biol. Macromol.*, 2024, **273**, 133204.
13 S. Wakekar, B. Jana, S. Yarramsetti, S. Ghosh, L. N. Patro, P. S. Maram, M. Shanmugam and C. Das, *J. Mater. Chem. A*, 2025, DOI: **10.1039/D5TA04374C**.
14 Y. Guo, W. Guan, C. Lei, H. Lu, W. Shi and G. Yu, *Nat. Commun.*, 2022, **13**, 1–7.
15 S. K. Shetty Ismayil, P. Nayak, Y. N. Sudhakar and I. M. Noor, *J. Energy Storage*, 2024, **95**, 112553.
16 Y. Chen, Y. Wang, Z. Li, D. Wang, H. Yuan, H. Zhang and Y. Tan, *Compos. Commun.*, 2021, **26**, 100774.
17 S. Ding, C. Fang, X. Wang and Z. Wang, *Polymer*, 2020, **186**, 121993.
18 R. Rahmawati, S. Nozaki, K. Kojio, A. Takahara, N. Shinohara and S. Yamasaki, *Polym. J.*, 2019, **51**, 265–273.
19 W. Jin, T. Mei, Y. Wang, W. Xu, J. Li, B. Zhou and B. Li, *Carbohydr. Polym.*, 2014, **99**, 270–277.
20 D. Kilburn, J. Claude, T. Schweizer, A. Alam and J. Ubbink, *Biomacromolecules*, 2005, **6**, 864–879.
21 H. Wang, C. Lin, X. Yan, A. Wu, S. Shen, G. Wei and J. Zhang, *J. Electroanal. Chem.*, 2020, **869**, 114156.
22 Y. Guo, W. Guan, C. Lei, H. Lu, W. Shi and G. Yu, *Nat. Commun.*, 2022, **13**, 1–6.
23 R. Sujanani, P. H. Nguyen, L. W. Gordon, J. T. Bamford, A. Zele, B. J. Pedretti, N. A. Lynd, R. J. Clément and R. A. Segalman, *ACS Macro Lett.*, 2025, **14**, 64–71.
24 N. Yadav, N. Yadav, M. K. Singh and S. A. Hashmi, *Energy Technol.*, 2019, **7**, 1–10.
25 S. B. Aziz, R. T. Abdulwahid, M. A. Brza, M. B. Ahmed, A. R. Murad, H. B. Tahir, R. M. Abdullah, J. M. Hadi and S. A. Hussen, *J. Energy Storage*, 2023, **71**, 108175.
26 N. M. Ghazali, N. F. Mazuki, M. H. Sulaiman, K. Aoki, Y. Nagao and A. S. Samsudin, *Solid State Ionics*, 2024, **414**, 116650.

